Zeeman Levels with Exotic Field Dependence in the High Field Phase of an $S = 1$ Heisenberg Antiferromagnetic Chain

M. Hagiwara,[1] Z. Honda,[2] K. Katsumata,[3] A. K. Kolezhuk,[4,5] and H.-J. Mikeska[4]
[1]*RIKEN (The Institute of Physical and Chemical Research), Wako, Saitama 351-0198, Japan*
[2]*Faculty of Engineering, Saitama University, Saitama 338-8570, Japan*
[3]*RIKEN Harima Institute, Mikazuki, Sayo, Hyogo 679-5148, Japan*
[4]*Institut für Theoretische Physik, Universität Hannover, Appelstraße 2, 30167, Hannover, Germany*
[5]*Institute of Magnetism, 36(B) Vernadskii Avenue, 03142 Kiev, Ukraine*
(Received 9 April 2003; published 22 October 2003)

We have performed electron spin resonance measurements over a wide frequency and magnetic field range on a single crystal of the $S = 1$ quasi-one-dimensional Heisenberg antiferromagnet $Ni(C_5H_{14}N_2)_2N_3(PF_6)$. We observed gapped excitation branches above the critical field H_c where the Haldane gap closes. These branches are analyzed by a phenomenological field theory using the complex-field ϕ^4 model. A satisfactory agreement between experiment and theory is obtained.

DOI: 10.1103/PhysRevLett.91.177601 PACS numbers: 76.50.+g, 75.10.Jm, 75.50.Ee

Recently, field-induced phenomena in quantum spin systems have attracted considerable interest. These include magnetization plateaus [1–3] and field-induced long-range order (LRO) [4–6]. Gapped one-dimensional (1D) spin systems subject to an external magnetic field strong enough to close the gap are driven into a new phase. When the system has XY or Heisenberg symmetry, this phase is critical and its low-energy physics is described by the Tomonaga-Luttinger liquid [7], whose elementary excitations are of the particle-hole type (spinon pairs). The high-energy physics which cannot be described using this picture has been recently investigated experimentally [8–10] as well as theoretically [11].

One-dimensional Heisenberg antiferromagnets (HAFs) with integer spin are typically gapped and have a disordered spin liquid singlet ground state [12]. The first excited state is a triplet and one of the Zeeman-split triplet branches goes down in the magnetic field. At some critical field H_c the gap closes, a qualitatively new ground state emerges, and magnetism recovers. Above H_c, a LRO is expected to occur in quasi-1D integer-spin HAFs owing to an interchain interaction. Such a field-induced LRO in the $S = 1$ quasi-1D HAF was found recently by specific heat measurements on a single crystal of $Ni(C_5H_{14}N_2)_2N_3(PF_6)$, abbreviated NDMAP [4,5]. Figure 1 shows the magnetic field versus the temperature phase diagram of NDMAP. The regions below and above the boundary denoted as $H_{LRO}(T)$ correspond to the Haldane and LRO phase, respectively. The critical field H_c in the present Letter is defined as H_{LRO} extrapolated to $T = 0$.

Quite recently, three distinct excitation branches were observed in inelastic neutron scattering (INS) experiments on NDMAP in the LRO phase above H_c for $H \parallel a$, and a satisfactory description within a phenomenological field theory was obtained [9]. This observation is remarkable since one expects two branches from the conventional spin-wave theory.

Electron spin resonance (ESR) is one of the powerful methods to investigate magnetic excitations, especially at low energies with a much better energy resolution than INS. In Ref. [13], we observed ESR signals in a single crystal of NDMAP and interpreted the results as the coexistence of 1D and 3D excitations, because no satisfactory description was available above H_c at that time.

In the present Letter we extend the ESR study of NDMAP to a much wider frequency range from which we obtain new results. A nontrivial field dependence of the resonance modes, very different from that expected from a conventional spin-wave theory, is observed. We compare the experimental results with model calculations based on the field theory used in the analysis of the recent INS experiments [9] and obtain good agreement with the theory.

First we summarize the crystal and magnetic properties of NDMAP. This compound crystallizes in the orthorhombic system (space group $Pnmn$) [14]. The Ni^{2+} ions are bridged by azido ions forming antiferromagnetic

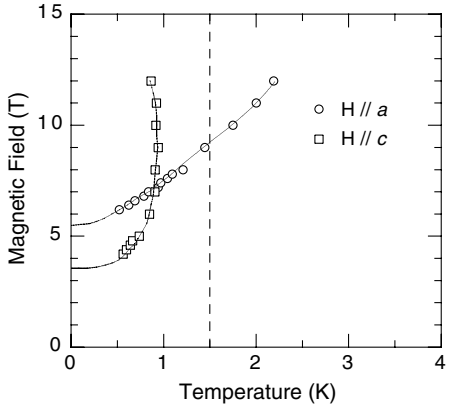

FIG. 1. The magnetic field versus temperature phase diagram of NDMAP; solid lines are guides to the eye (figure from [4]). The ESR measurements were performed along the dashed line.

chains along the c axis. All the Ni sites in a chain are crystallographically equivalent, so that no staggered components of the magnetic moments are retained in the ground state below H_c. The physics in NDMAP is thus essentially different from that in other typical Haldane materials $Ni(C_2H_8N_2)_2NO_2(ClO_4)$ (abbreviated NENP) and $Ni(C_3H_{10}N_2)_2NO_2(ClO_4)$ (abbreviated NINO), extensively studied by ESR [15]. These studies showed that the Haldane gap did not close at H_c due to a staggering of the local crystal fields for Ni^{2+} [16,17]. Consequently, no clear transition from the disordered to LRO phase is observed and the ESR transitions from the ground state are always allowed.

From the analysis of the magnetic susceptibility, the following values are obtained [4]: $J = 30.0$ K, $D/J = 0.3$, $g_{\|} = 2.10$, and $g_{\perp} = 2.17$, where J is the intrachain exchange interaction constant, and $g_{\|}$ and $g_{\perp}$ are the g values parallel and perpendicular to the chain, respectively. From the INS measurements done on single crystals of deuterated NDMAP [18] the following parameters were determined: $J = 33.1$ K, $J'_x = 4.1 \times 10^{-3}$ K, $J'_y = 2.1 \times 10^{-2}$ K, and $D = 8.1$ K, where J'_x and J'_y are the interchain exchange interactions along the a and b axes, respectively.

The single crystals of NDMAP were grown in the manner described in Ref. [4]. The ESR measurements were performed using a millimeter vector network analyzer with extensions up to about 700 GHz from AB Millimeter, France, and a superconducting magnet up to 16 T from Oxford Instruments, United Kingdom. We performed the ESR measurements in $H \| a$ and $H \| c$ geometries at the lowest temperature available with our spectrometer (1.5 K). Faraday and Voigt configurations were used for $H \| a$ and $H \| c$, respectively. As shown in Fig. 1, the external magnetic field of ≈ 9 T for $H \| a$ brings the system into the LRO phase at 1.5 K.

Figure 2 shows a typical example of ESR spectra observed for $H \| a$ and $H \| c$. The signal at about 13.5 T for $H \| a$ comes from the LRO phase. We observed comparable ESR intensities for Faraday and Voigt configurations. In Fig. 3(a), the resonance frequencies for $H \| a$ as a function of magnetic field are shown with solid circles. We also plot with solid squares the gap energies obtained from the recent INS measurements at 30 mK [9]. In the figure, the vertical dashed line and the vertical dotted line denote H_c and H_{LRO} at 1.5 K, respectively. It is obvious that the slope of the branches changes at H_c and not at H_{LRO}. It should be remarked that a similar change of slope was observed in the quasi-1D material NENC [8] and in the 3D weakly coupled dimer system $TlCuCl_3$ [10,19]. The observed neutron data below H_c represent the magnon triplet split by the single ion anisotropy in the Haldane phase. Below H_c, only temperature-induced ESR transitions between the magnon branches are allowed. Only one ESR line, corresponding to the transition between the lowest two branches, was observed near the critical field below H_c. Above H_c, three ESR lines were observed. Their positions coincide with the INS data for the gaps at $q = \pi$, confirming that they correspond to the transitions from the ground state. It is worthwhile to note that these lines appear at $H > H_c$ and not at $H > H_{LRO}$ as one would naively expect, and that there is no anomaly in

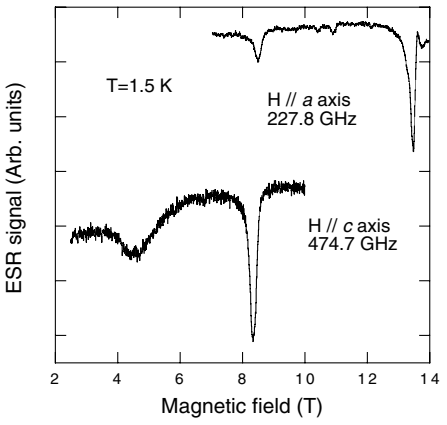

FIG. 2. An example of ESR spectra for $H \| a$ and $H \| c$ obtained at 1.5 K.

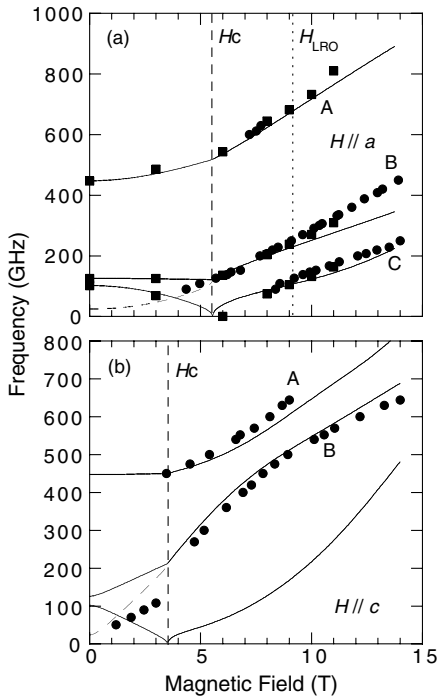

FIG. 3. The ESR resonance fields are plotted with solid circles in the frequency versus magnetic field plane for (a) $H \| a$ (the field perpendicular to the chain) and (b) $H \| c$ (the field parallel to the chain), respectively. The dashed vertical line is the critical field H_c at $T = 0$ K. The solid lines are fits based on the field-theoretical approach. The thin dashed line below H_c denotes transition between the lowest two excited states. In the upper panel, the solid squares are taken from the neutron inelastic measurements [9] at the wave vector $q = \pi$. The dotted vertical line denotes the boundary between the disordered and the LRO phases at $T = 1.5$ K (see Fig. 1).

the behavior of resonance lines at H_{LRO}. Indeed, the gap of the lowest magnon branch at $q = \pi$ closes at $H = H_c$ at any temperature, causing "condensation" of $q = \pi$ magnons into the ground state at $H > H_c$. The amplitude of the $q = \pi$ component becomes nonzero immediately above H_c, making the ESR transitions from the ground state to the excited ones at $q = \pi$ possible. The transversal staggered LRO, however, emerges only at the higher field H_{LRO}, because the phase coherence of the condensate wave function, directly related to the LRO, is destroyed by thermal fluctuations in the field range $H_c < H < H_{\mathrm{LRO}}$. Transitions at $q = \pi$ require finite amplitude of the $q = \pi$ component but not phase coherence. The amplitude becomes finite at H_c but shows no peculiarity at H_{LRO} when phase coherence sets in; therefore, the ESR signal appears at $H = H_c$ and continues without essential change through H_{LRO}.

Figure 3(b) shows a frequency versus field plot of the resonance point for $H \parallel c$. As in the $H \parallel a$ case, we observed only one resonance line below H_c which corresponds to the temperature-induced transitions between the lowest two magnon branches. Above H_c, two ESR lines were observed. For this geometry, there is no LRO at 1.5 K, so that the measurements were conducted completely outside the LRO phase. One of the remarkable features in this figure is a change in slope at about 7 T, far above the critical field $H_c \simeq 3.5$ T, resulting from an avoided crossing between the two branches (see below).

Now, we compare the experimental results with theoretical calculations using a field-theoretical model [9] similar to that proposed for dimerized $S = \frac{1}{2}$ chains in Ref. [20]. It is a Ginzburg-Landau-type theory written in terms of a *complex* triplet field $\boldsymbol{\phi} = \boldsymbol{A} + i\boldsymbol{B}$ which is assumed to be small, $|\boldsymbol{\phi}| \ll 1$. For a dimerized $S = \frac{1}{2}$ system, the field $\boldsymbol{\phi}$ describes the dimer wave function $|\boldsymbol{\phi}\rangle = (1 - |\boldsymbol{\phi}|^2)^{1/2}|s\rangle + \sum_{a=x,y,z}\phi_a|t_a\rangle$, where $|s\rangle$ and $|t_a\rangle$ are the singlet and three triplet states of the dimer; it is a continuum analog of the bond boson description used in [19]. The uniform and staggered magnetizations are given by $\boldsymbol{M} = (\boldsymbol{\phi}^* \times \boldsymbol{\phi})$ and $\boldsymbol{L} = (\boldsymbol{\phi}^* + \boldsymbol{\phi})(1 - |\boldsymbol{\phi}|^2)$, respectively. The effective Lagrangian density in the continuum limit has the following form:

$$\begin{aligned}\mathcal{L} = {} & \hbar(\boldsymbol{A} \cdot \partial_t \boldsymbol{B} - \boldsymbol{B} \cdot \partial_t \boldsymbol{A}) - (1/2)v^2(\partial_x \boldsymbol{A})^2 \\ & - \sum\{m_\alpha A_\alpha^2 + \tilde{m}_\alpha B_\alpha^2\} + 2\boldsymbol{H} \cdot (\boldsymbol{A} \times \boldsymbol{B}) \\ & - \lambda(\boldsymbol{A}^2)^2 - \lambda_1(\boldsymbol{A}^2\boldsymbol{B}^2) - \lambda_2(\boldsymbol{A} \cdot \boldsymbol{B})^2. \qquad (1)\end{aligned}$$

This model, though derived for dimerized $S = \frac{1}{2}$ chains, may also be used for other gapped 1D systems which are in the same universality class, particularly for $S = 1$ Haldane chains. In this case, the quantities m_α, $\tilde{m}_\alpha$, and λ_i should be treated as phenomenological parameters; the direct microscopic justification of this model for $S = 1$ chains is the subject of ongoing work. The spatial derivatives of $\boldsymbol{B}$ are omitted in (1) because they appear only in terms which are of the fourth order in $\boldsymbol{A}$ and $\boldsymbol{B}$. By integrating out the "slave" $\boldsymbol{B}$ field one obtains an effective real-field theory which generalizes previous theoretical approaches in that it deals successfully with anisotropic chains both below and above H_c: For isotropic $\tilde{m}_\alpha = \tilde{m}$ and simplified interaction term $\lambda_{1,2} = 0$ (1) yields the theory of Affleck [21]. Another special case $m_\alpha = \tilde{m}_\alpha$ leads to the spectra which for $H < H_c$ exactly coincide with those obtained in the approach of Tsvelik [22] involving three massive Majorana fields, and also with the perturbative formulas [23]; under additional assumption $\lambda_{1,2} = 0$ the theory becomes equivalent to that of Mitra and Halperin [16] who postulated a bosonic Lagrangian to match Tsvelik's results for the gaps below H_c.

The solid lines in Figs. 3(a) and 3(b) represent the best fit of the calculated energy gaps at $q = \pi$ to the experimental data. This fit is obtained using the following set of model parameters (all values in meV): $m_a = 0.5$, $m_b = 0.8$, $m_c = 5.29$, $\tilde{m}_a = 0.353$, $\tilde{m}_b = 0.342$, $\tilde{m}_c = 0.647$, $\lambda = 1$, $\lambda_1 = -\lambda_2 = 0.13$. We obviously see a change in slope of each excited branch and reopening the energy gap of the lowest branch at H_c. Below $H_c \simeq 5.5$ T in Fig. 3(a), three excitation branches are in good agreement with the neutron data. The ESR transitions from the ground to the excited states at $q = \pi$ are forbidden because no staggered component exists in the ground state of this compound. In both figures, the ESR resonance points appear only near H_c, because these correspond to the transition between the excited states and the intensity is related to the population of the excited states at 1.5 K. The thin dashed line in each figure indicates the transition between the lowest two magnon branches at $q = \pi$. For those temperature-induced transitions, the agreement between experiment and calculation is satisfactory for $H \parallel a$ and is not good for $H \parallel c$. Above H_c, the calculated branches are close to the experimental data near H_c but deviate from them at high fields. This is probably because the theory is applicable only for the state with a small staggered order and thus only for fields which are not too far above H_c.

In these calculations, we have taken into account the tilting of the crystal field axis of the Ni^{2+} ions from the crystallographic c axis. The tilting angle is 15.9°. In Fig. 3(b), a change in slope at about 7 T observed in the A and B branches is reproduced in the calculation. Because of the tilting of the crystal field axis, the external magnetic field applied parallel to the c axis mixes the wave functions of A and B branches. The origin of this change in slope is different from that of the changes visible near the critical field. The observed ESR line below H_c in Fig. 3(b) deviates from the expected thin dashed line, although satisfactory agreement is obtained for $H \parallel a$; further theoretical and experimental work is required to clarify the reason for this discrepancy concerning temperature-induced lines. For $H \parallel c$, we did not observe ESR signals corresponding to the lowest calculated mode above H_c; we speculate that this is caused by a

strong damping of the lowest magnon mode due to the interaction with domain walls, because our measurement was done at a high temperature. A similar problem arose in INS measurements [24] in the $H \parallel a$ geometry, and only after lowering the temperature to 30 mK the mode was successfully observed [9]. The damping should be much stronger in the $H \parallel c$ geometry, due to the lower energy and, respectively, higher density of domain walls.

Remarkably, the observed field dependence of the ESR modes for both geometries is very different from that expected from a conventional spin-wave theory. Indeed, in a conventional (classical) antiferromagnet with easy-plane anisotropy D and external magnetic field H applied in the easy plane, there are two resonance modes with the energies $\varepsilon_1 = g\mu_B H$ and $\varepsilon_2 = 2S\sqrt{2DJ}$. For H perpendicular to the easy plane, one would classically expect to see one field-dependent resonance mode with the energy $\varepsilon_2' = \sqrt{(g\mu_B H)^2 + \varepsilon_2^2}$, the energy of the other mode being zero. We have observed and described theoretically completely different behaviors above H_c for both directions: in the $H \parallel a$ case (in-plane geometry) the lowest two energy modes increase approximately as $g\mu_B H$ and the highest energy mode as $2g\mu_B H$, and for $H \parallel c$ we observe the (avoided) crossing of two modes whose energies behave roughly as $g\mu_B H$ and $2g\mu_B H$.

In conclusion, we have performed ESR measurements on a single crystal of the $S = 1$ quasi-one-dimensional Heisenberg antiferromagnet NDMAP and observed ESR spectra corresponding to the gapped state above the critical field where the Haldane gap closes. For $H \parallel a$ our ESR data above H_c, taken at $T = 1.5$ K, agree very well with those from inelastic neutron scattering [9] obtained at much lower temperature, and the observed resonances are not affected by the boundary of the long-range-ordered phase at $H \simeq 9$ T. For $H \parallel c$ we observed a change in slope of the ESR line resulting from an avoided crossing between the two modes having nontrivial slopes H and $2H$. The observed field dependence of the magnon modes for both geometries $H \parallel a$ and $H \parallel c$ is very different from that expected from a conventional spin-wave theory. Model calculations based on the field-theoretical approach have satisfactorily reproduced most of the features of the observation on a quantitative level.

We thank A. Zheludev for enlightening discussions. This work was in part supported by the Molecular Ensemble research program from RIKEN and the Grant-in-Aid for Scientific Research on Priority Areas (B): Field-Induced New Quantum Phenomena in Magnetic Systems (No. 13130203) from the Japanese Ministry of Education, Culture, Sports, Science and Technology, and by Grant No. I/75895 "Low-dimensional magnets in high magnetic fields" from Volkswagen-Stiftung.

[1] Y. Narumi, M. Hagiwara, R. Sato, K. Kindo, H. Nakano, and M. Takahashi, Physica (Amsterdam) **246B**, 509 (1998).
[2] W. Shiramura, K. Takatsu, B. Kurniawan, H. Tanaka, H. Uekusa, Y. Ohashi, K. Takizawa, H. Mitamura, and T. Goto, J. Phys. Soc. Jpn. **67**, 1548 (1998).
[3] H. Kageyama, K. Yoshimura, R. Stern, N.V. Mushnikov, K. Onizuka, M. Kato, K. Kosuge, C. P. Slichter, T. Goto, and Y. Ueda, Phys. Rev. Lett. **82**, 3168 (1999).
[4] Z. Honda, H. Asakawa, and K. Katsumata, Phys. Rev. Lett. **81**, 2566 (1998).
[5] Z. Honda, K. Katsumata, Y. Nishiyama, and I. Harada, Phys. Rev. B **63**, 064420 (2001).
[6] Y. Chen, Z. Honda, A. Zheludev, C. Broholm, K. Katsumata, and S. M. Shapiro, Phys. Rev. Lett. **86**, 1618 (2001).
[7] R. Chitra and T. Giamarchi, Phys. Rev. B **55**, 5816 (1997).
[8] M. Orendác, S. Zvyagin, A. Orendácová, M. Seiling, B. Lüthi, A. Feher, and M.W. Meisel, Phys. Rev. B **60**, 4170 (1999).
[9] A. Zheludev, Z. Honda, C. L. Broholm, K. Katsumata, S. Shapiro, A. Kolezhuk, S. Park, and Y. Qiu, cond-mat/0301424.
[10] Ch. Rüegg, N. Cavadini, A. Furrer, K. Krämer, H. U. Güdel, P. Vorderwisch, and H. Mutka, Appl. Phys. A **74**, S840 (2002).
[11] A. K. Kolezhuk and H.-J. Mikeska, Phys. Rev. B **65**, 014413 (2002); Prog. Theor. Phys. Suppl. **145**, 85 (2002).
[12] F. D. M. Haldane, Phys. Lett. A **93**, 464 (1983); Phys. Rev. B **25**, 4925 (1982).
[13] Z. Honda, K. Katsumata, M. Hagiwara, and M. Tokunaga, Phys. Rev. B **60**, 9272 (1999).
[14] M. Monfort, J. Ribas, X. Solans, and M. F. Bardia, Inorg. Chem. **35**, 7633 (1996).
[15] W. Lu, J. Tuchendler, M. von Ortenberg, and J. P. Renard, Phys. Rev. Lett. **67**, 3716 (1991); T. M. Brill, J. P. Boucher, L. C. Brunel, J. P. Renard, and M. Verdaguer, Physica (Amsterdam) **204B**, 303 (1995); M. Sieling, U. Löw, B. Wolf, S. Schmidt, S. Zvyagin, and B. Lüthi, Phys. Rev. B **61**, 88 (2000).
[16] P. P. Mitra and B. I. Halperin, Phys. Rev. Lett. **72**, 912 (1994).
[17] T. Sakai and H. Shiba, J. Phys. Soc. Jpn. **63**, 867 (1994).
[18] A. Zheludev, Y. Chen, C. L. Broholm, Z. Honda, and K. Katsumata, Phys. Rev. B **63**, 104410 (2001).
[19] M. Matsumoto, B. Normand, T. M. Rice, and M. Sigrist, Phys. Rev. Lett. **89**, 077203 (2002).
[20] A. K. Kolezhuk, Phys. Rev. B **53**, 318 (1996).
[21] I. Affleck, Phys. Rev. B **41**, 6697 (1990); Phys. Rev. B **43**, 3215 (1991).
[22] A. M. Tsvelik, Phys. Rev. B **42**, 10 499 (1990).
[23] O. Golinelli, Th. Jolicoeur, and R. Lacaze, Phys. Rev. B **45**, 9798 (1992); J. Phys. Condens. Matter **5**, 7847 (1993); L.-P. Regnault, I. A. Zaliznyak, and S.V. Meshkov, J. Phys. Condens. Matter **5**, L677 (1993).
[24] A. Zheludev, Z. Honda, Y. Chen, C. Broholm, and K. Katsumata, Phys. Rev. Lett. **88**, 077206 (2002).